

Sustainable Food Technology

Accepted Manuscript

This article can be cited before page numbers have been issued, to do this please use: L. M and S. Karthick Raja Namasivayam, *Sustainable Food Technol.*, 2025, DOI: 10.1039/D5FB00833F.



This is an Accepted Manuscript, which has been through the Royal Society of Chemistry peer review process and has been accepted for publication.

Accepted Manuscripts are published online shortly after acceptance, before technical editing, formatting and proof reading. Using this free service, authors can make their results available to the community, in citable form, before we publish the edited article. We will replace this Accepted Manuscript with the edited and formatted Advance Article as soon as it is available.

You can find more information about Accepted Manuscripts in the [Information for Authors](#).

Please note that technical editing may introduce minor changes to the text and/or graphics, which may alter content. The journal's standard [Terms & Conditions](#) and the [Ethical guidelines](#) still apply. In no event shall the Royal Society of Chemistry be held responsible for any errors or omissions in this Accepted Manuscript or any consequences arising from the use of any information it contains.

Sustainable Spotlight Statement

This research introduces a sustainable and biocompatible nanoencapsulation strategy using chitosan and *Clitoria ternatea* extract to enhance the functionality, stability, and survivability of the probiotic strain *Lactobacillus acidophilus*. The developed CT-CS-LA-NC system integrates natural, renewable materials to improve probiotic tolerance under acidic and bile conditions, strengthen antibacterial and antioxidant properties, and extend storage stability without synthetic additives. By leveraging green biopolymers and plant-derived bioactives, this study contributes to the advancement of environmentally responsible probiotic delivery systems. The approach aligns with sustainable food innovation goals by promoting resource-efficient, safe, and functional probiotic formulations suitable for next-generation functional foods and nutraceuticals.



1 **Chitosan based ecofriendly nanoencapsulation formulation of *Clitoria ternatea* extract**
2 **coated bacterial probiotic strain *Lactobacillus acidophilus*: A Sustainable Approach to**
3 **Improve Probiotic Functionality, Stability, and Tolerance**

4 **M. Lavanya¹, S. Karthick Raja Namasivayam^{1*}**

5 ¹Centre for Applied Research, Saveetha School of Engineering, Saveetha institute of Medical
6 and Technical Sciences (SIMATS), Chennai - 602105, Tamil Nadu, India.

7
8
9
10
11
12
13
14 Corresponding Author*

15 Dr.S. Karthick Raja Namasivayam
16 Professor
17 Centre for Applied Research
18 Saveetha School of Engineering
19 Saveetha Institute of Medical and Technical Sciences (SIMATS)
20 Chennai – 602105
21 Phone: +919842441198
22 Mail: biologiask@gmail.com
23

24
25
26
27
28
29
30
31



32 Abstract

33 In this study, a sustainable nanoencapsulation formulation of *Clitoria ternatea* extract-
34 coated bacterial probiotic strain *Lactobacillus acidophilus* using nanoscale chitosan (CT-CS-
35 LA-NC) was developed to enhance probiotic functionality, stability, and tolerance. The
36 structural and functional characteristics of the nanoencapsules were analyzed using Scanning
37 Electron Microscopy (SEM), Fourier Transform Infrared Spectroscopy (FTIR), and
38 Thermogravimetric Analysis (TGA). These analyses confirmed that the CT-CS-LA-NC
39 nanoencapsules were nanoscale in size, highly thermostable, and exhibited strong interactions
40 among the polymer matrix, bacterial cell surface components, and plant extract. The
41 encapsulation efficiency was found to be 98.43%, indicating effective preservation of viable
42 probiotic cells during the encapsulation process. The antibacterial activity of CT-CS-LA-NC
43 demonstrated significant inhibition against *Escherichia coli* and *Bacillus subtilis*. Antioxidant
44 assessment revealed a free radical scavenging activity of 48.2 ± 1.32 %. Under simulated
45 gastric conditions (pH 2.5 and 3.5), the survivability of free and nanoencapsulated *L.*
46 *acidophilus* showed notable differences after 36 hours. The encapsulated cells exhibited a
47 higher survival rate of $60.93 \pm 0.68\%$ at pH 2.5, compared to only $21.29 \pm 0.13\%$ for free cells.
48 Similarly, under bile tolerance conditions, encapsulated cells showed a survivability of 39.46
49 $\pm 0.68\%$ at pH 2.5. Storage stability studies at 4°C over 28 days revealed a rapid decline in the
50 viability of free *L. acidophilus* cells, whereas CT-CS-LA-NC encapsulated cells maintained
51 94% viability after 7 days and 52% after 28 days. Molecular docking analysis using CB-Dock
52 demonstrated strong binding affinities between anthocyanin, lactic acid, and chitosan ligands
53 with gut-associated proteins such as O-GlcNAcase (7K41) and S-layer associated protein
54 (SlpA) (8AE1), showing binding energies of -9.4 and -9.6 kcal/mol, respectively. Overall, the
55 biocompatible and environmentally safe CT-CS-LA-NC formulation significantly improved
56 probiotic stability during storage, enhanced survivability under harsh gastrointestinal
57 conditions, and prolonged probiotic shelf life. These findings highlight its potential application
58 as a sustainable ingredient for functional foods and nutraceutical formulations.

59

60 **Keywords:** *Lactobacillus acidophilus*, Probiotics, Nanoencapsulation, *Clitoria ternatea*,
61 Chitosan, acid tolerance, storage stability

62

63



64
65
66
67
68
69
70
71
72
73
74
75
76
77
78
79
80
81
82
83
84
85
86
87
88
89
90

View Article Online
DOI: 10.1039/D5FB00833F

Highlights

- Sustainable chitosan nanoencapsulation enhanced *L. acidophilus* functionality.
- CT-CS-LA-NC showed 98.43% encapsulation efficiency with high cell preservation.
- Strong antibacterial and antioxidant activities improved probiotic performance.
- Enhanced acid and bile tolerance increased *L. acidophilus* survivability.
- Excellent storage stability supports use in sustainable functional foods.



91

92 **1. INTRODUCTION**

93 Food spoilage is a significant issue affecting the economy and brand reputation of
94 manufacturers. The food preservation and processing industry also seeks alternatives to
95 conventional preservatives [1]. The food industry is utilizing probiotic microorganisms,
96 specifically lactic acid bacteria and bifidobacteria, as bio preservatives to create healthy and
97 safe food products [2]. These probiotics act as bio-preservatives, balancing beneficial and
98 harmful bacteria in plant-based foods [3,4]. FDA and WHO define probiotics as “live
99 microorganisms which when administered in adequate amounts confer a health benefit on the
100 host,” which includes genera like *Saccharomyces*, *Bifidobacterium*, *Lactobacillus*,
101 *Enterococcus*, *Bacillus*, *Escherichia*, and *Streptococcus* [5,6].

102 Probiotics compete with harmful bacteria for adhesion sites, preventing colonization.
103 They strengthen the intestinal barrier, reducing permeability and preventing harmful
104 substances from entering the bloodstream [7]. Additionally, probiotics produce antimicrobial
105 substances that inhibit pathogenic bacteria growth and can modulate the immune system to
106 enhance defence mechanisms. Some probiotics also contribute to neurotransmitter synthesis,
107 and influences the gut-brain communication [8]. Selecting the right probiotic strain is crucial
108 for specific conditions. The amount consumed, formulation, and storage conditions are crucial
109 for their effectiveness. Probiotics must survive the acidic stomach environment and small
110 intestine bile. Quality control and shelf-life also impact the efficacy of probiotic products.
111 Combining probiotics with prebiotics or other beneficial compounds can enhance their effects
112 [7,9]. Among the crucial probiotic characteristics of *Lactobacillus acidophilus* that have been
113 demonstrated in vitro and belong to the first group are antibiotic production, bile susceptibility,
114 adaptability to low pH, adhere to human colon cells, lactase activity, and stability of the
115 product. The latter group includes the general probiotic advantages observed in feeding studies



116 at the animal level, such as immune response regulation, lowering serum cholesterol,
117 improving lactose metabolism, and preventing or treating infections. When combined with
118 chitosan-based antimicrobial preservatives, these probiotics can significantly enhance shelf life
119 and food safety and maintain the quality of food products, presenting a natural and sustainable
120 alternative to traditional preservation methods [10]. Among probiotic bacteria, *Lactobacillus*
121 *acidophilus* is one of the more efficient types. Because of its advantageous properties, studies
122 have indicated that it can be added to fermented foods. For *Lactobacillus acidophilus* to be
123 effective as probiotics, it must adapt to the intestinal environment of the host and be viable and
124 physiologically active at the target site in the host [11].

125 Encapsulated probiotics are used in various products, and they are used to protect cores
126 from degradation, reduce evaporation, improve material handling, and enhance the stability of
127 the active ingredients. These benefits make encapsulated probiotics an essential component in
128 the formulation of dietary supplements and functional foods [12]. Encapsulation methods
129 involve trapping or adhering drugs to a matrix or surface, or bonding drugs to the material.
130 Molecular weight, and stability, play crucial roles in determining their effectiveness and safety.
131 Larger molecules may pose challenges, and interactions between drugs and capsules influence
132 encapsulation. Various capsule production methods have been developed, influenced by factors
133 like particle size, reproducibility, and final product stability [13]. Alginate is the most widely
134 used biopolymer for microencapsulation because it is inexpensive, non-toxic, forms gentle
135 matrices with calcium chloride, and is easy to entrap living microbial cells. It is also a food
136 additive that is widely acknowledged and can be used in food without any harmful effects. Its
137 low stability in the presence of chelating agents and in acidic environments below pH 2 restricts
138 its application [14]. Coating alginate beads with chitosan enhances the stability and vitality of
139 encapsulated probiotic microbes. The colon's microbiota breaks down chitosan and solubilizes
140 alginate gel by retaining calcium ions [15].



141 Probiotic foods are also sources of other nutritional compounds, such as antioxidants,
142 fibre, unsaturated fatty acids, minerals, or vitamins and offer synergistic effects to health [16].
143 *Clitoria ternatea* is a flower is rich in antioxidants, flavonoids, and phenolic compounds, with
144 antimicrobial properties. It is used in nanoencapsulation to improve the stability and
145 bioavailability of bioactive compounds, protect sensitive ingredients from oxidation, and
146 enhance controlled nutrient release in food and pharmaceutical applications [17]. Compared to
147 synthetic encapsulating agents, *C. ternatea* offers natural antioxidant protection, higher
148 encapsulation efficiency for anthocyanins, and better bioavailability than conventional
149 microencapsulation techniques [18]. Although *Clitoria ternatea* has been investigated for its
150 antioxidant and antibacterial characteristics, its utilization in chitosan-alginate-based
151 nanoencapsulation for probiotic stabilization and ecotoxicity evaluation is insufficiently
152 reported. In this study, the viability of *L. acidophilus* with probiotic qualities was examined,
153 along with the isolation and encapsulation of *C. ternatea* extract coated chitosan- *L.acidophilus*
154 Nano-encapsule (CT-CS-LA-NC). Poly dispersive index, zeta potential, thermogravimetric
155 Analysis (TGA), and Scanning Electron Microscopy (SEM), fourier Transform Infrared
156 Spectroscopy (FTIR), encapsulation efficiency were used to examine the structural and
157 functional properties followed by the antioxidant property, gastrointestinal survivability and
158 storage stability of probiotic nanoencapsules. The environmental compatibility was evaluated
159 through ecotoxicity profiling and molecular interaction modeling.

160 **2.Materials and methods**

161 **2.1 Reagents and chemicals**

162 All reagents and chemicals for nano-encapsule preparation and other biological assays
163 including protein profiling study were purchased from Sigma. Hi-media, India, provided the
164 culture medium used for the microbiological analysis (extra pure analytical grade). All the
165 chemicals were obtained with high purity and it was used without any further purification.



166 **2.2 Isolation of *Lactobacillus acidophilus* from curd**

View Article Online
DOI: 10.1039/D5FB00833F

167 The probiotic strain used in this study was isolated from fresh homemade curd prepared
168 from cow milk obtained from local milk store in Purasawalkam, Chennai. The sample was
169 collected in a sterile flask, and stored under refrigerated conditions (4°C). The initial pH of the
170 curd sample was measured to be 4.7. Initially, 10 g of curd sample was homogenised in 90 mL
171 of sterile distilled water to make a 10⁻¹ (w/v) stock suspension. Serial dilutions were performed
172 on this suspension by transferring 1 mL of the preceding dilution into 9 mL of sterile distilled
173 water to generate a range of 10⁻² to 10⁻⁵. Then, 0.1 mL of each serially diluted sample was
174 poured into already pre-solidified MRS agar and incubated at 37 °C for 24 hours with constant
175 homogenous shaking under aerobic conditions. The bacterial isolates were purified using the
176 streak plate method and kept for four weeks at 4°C on agar slants until characterisation. Gram
177 stain and acid production tests were used to further analyse the isolate's cellular morphology
178 and staining properties [19].

179 **2.3 Identification of probiotic strain**

180 The isolated *Lactobacillus* species is identified using morphological (Gram staining,
181 spore test, and motility test), biochemical (indole production test and catalase test), and
182 molecular characterization (16S rRNA sequencing) for the identification of lactic acid bacteria
183 isolates. Plates with white and creamy colonies (presumptive for LAB) were selected and
184 purified through three successive transfers on MRS medium [20].

185 **2.3.1 16S rRNA sequencing analysis**

186 Further confirmation of bacterial strain was identified by 16S rRNA sequencing.
187 Genomic DNA prepared using universal primers, and PCR amplification of 16S rRNA was
188 carried out. PCR products were sequenced using universal primers. PCR reaction mixture (50
189 µl) comprising 5 µl of dNTPs, 1 µl of each primer rD1 and fD1, 1 µl of the extracted DNA, 5
190 µl of PCR buffer and 1 µl of Taq DNA polymerase, was used to amplify the 16S rRNA gene.



191 PCR amplicons and a heat cycler were used for the amplification process. The 16S rRNA gene
192 sequence reported in this study was identified with NCBI sequences. After the sequences were
193 aligned, MEGA version 4.0 was used to create a phylogenetic tree [21].

194 **2.3.2 Viable inoculum preparation of *L. acidophilus***

195 For inoculum preparation, the slant culture of *Lactobacillus* was inoculated in the
196 sterilized MRS broth (pH 6.2) at 37 °C for 24 h. The homogenised suspension was then
197 centrifuged for 10 minutes at 10,000 rpm. The biomass that was obtained from *L. acidophilus*
198 centrifuged and rinsed with 0.1 M phosphate-buffered saline. The cells were then resuspended
199 in Phosphate Buffer Saline. The washed cells served as the inoculum source [22].

200 **2.4 Preparation of *C. ternatea* extract coated chitosan- *L. acidophilus* Nano-encapsule** 201 **(CT-CS-LA-NC)**

202 *C. ternatea* (butterfly pea flowers) was purchased from the local retail outlets. They
203 were subjected to a pretreatment process by double washing with running tap water and
204 distilled water to remove impurities. Ten grams of butterfly pea flower petals were
205 homogenized and soaked in 100 mL of distilled water. The mixture was then placed on a rotary
206 shaker for 72 hours. After this period, the suspension was gently shaken and filtered through
207 filter paper to remove the solids. The filtered crude extract, was concentrated using a rotary
208 evaporator set at 50°C (TOP-300RE) to a constant weight and the resulting dry mass yield was
209 measured as 5.059 mg/mL the concentration was determined by dividing the final mass by the
210 initial volume using a gravimetric method [22]. The concentrated extract from the butterfly pea
211 flower petals was collected in screw-cap vials for the formulation of nano-encapsule. The
212 qualitative analysis of aqueous *C. ternatea* flower extract was assessed by the standardized
213 method reported by Chakraborty et al. (2017).

214 In a typical procedure, nano-encapsulated chitosan and probiotic (*Lactobacillus*) with
215 plant extract (*C. ternatea*) was formulated. 25 mL of 1.2% sodium alginate and 1 mL of *C.*



216 *ternatea* extract and 0.5 mL of probiotic suspension (CT-CS-LA-NC) were drawn into a 10
217 mm diameter Pasteur pipette. These were then carefully dispensed drop by drop into a solution
218 containing 100 mL of 10% CaCl₂ and 1 mL of Tween 20, forming beads. Droplets were
219 immersed in a calcium chloride solution for 30 minutes. The beads were retrieved, rinsed twice
220 with sterile water, and blotted in a petri dish to remove any remaining water, resulting in
221 surface-dried beads [24]

222 2.5 Encapsulation efficiency

223 The encapsulation efficiency (EE) of coating materials refers to their ability to hold or
224 encapsulate core materials within the capsule, and it is a key feature of wall materials. After
225 the CT-CS-LA-NC beads dissolved, the encapsulated probiotic cells were counted directly to
226 determine the encapsulation efficiency (EE). 1 mL of the initial probiotic mixture was plated
227 onto MRS agar after being serially diluted in sterile phosphate-buffered saline (PBS, pH 7.2).
228 After 48 hours of incubation at 37°C, the initial cell concentration (Ni) was calculated by
229 counting the colony-forming units (CFU) on the plates. For the encapsulated cells, 1 g of CT-
230 CS-LA-NC beads was homogenized using a sterile glass homogenizer and added to 9 mL of
231 sterile PBS, and then 1 mL of the solution was serially diluted in sterile PBS and plated on
232 MRS agar. The colonies were counted after 48 hours of incubation at 37°C to determine the
233 final cell concentration (Nf) [25]. The encapsulation efficiency was calculated using the
234 following formula:

$$235 \quad EE (\%) = (Nf/Ni) \times 100$$

236 where Ni is the initial cell concentration before encapsulation and Nf is the final cell
237 concentration after encapsulation.

238 2.6 Characterization of CT-CS-LA-NC

239 The structural and functional properties of the nanoencapsule were determined by using
240 appropriate analytical techniques. The findings provided essential insights into the capsule's



241 stability and release mechanisms, facilitating prospective uses in preservation. The data
242 indicate that the nanoencapsule may improve efficacy while minimizing side effects.

243 **2.6.1 Particle Size and Polydispersity Index (PDI)**

244 The Dynamic Light Scattering (DLS) method was used to measure the particle size and
245 Polydispersity Index (PDI) using a Malvern Zetasizer Nano ZS90 (Malvern Instruments Ltd.,
246 Worcestershire, UK). To obtain the ideal scattering intensity, all samples were diluted 1:100
247 with distilled water before analysis. Measurements were conducted in triplicate at a regulated
248 temperature of $25\pm 2^\circ\text{C}$, with the detector oriented at a 90° scattering angle. The Z-average
249 diameter (mean particle size) and PDI were determined by averaging the measurements done
250 in triplicate [26].

251 **2.6.2 Zeta Potential (ZP) Analysis**

252 The zeta potential of solid lipid nanoparticles was measured using the Malvern
253 Zetasizer Nano ZS90 (Malvern Instruments Ltd., Worcestershire, UK) at a temperature of 25
254 $\pm 2^\circ\text{C}$. This apparatus measures the zeta potential using the electrophoretic mobility of the
255 particles by combination of two measurement methods like electrophoresis and laser Doppler.
256 It shows that the physical stability of the SLNs is predicted. Prior to measurement, each sample
257 was diluted in distilled water, pH was maintained at 7.0 and the results were calculated by
258 average measurements in triplicate [26].

259 **2.6.3 Fourier Transform Infrared Spectroscopy**

260 Functional groups were recorded by FTIR, Thermo Fisher Scientific NICOLET-iS50
261 spectrophotometer with a micro attenuated total reflectance (ATR) accessory, using a diamond
262 disc as an internal reflection element.

263 **2.6.4 Scanning Electron Microscopy (SEM)**



264 The surface morphology of the freeze-dried nano-encapsules were analysed using a
265 scanning electron microscope (SEM). This analysis was performed with the assistance of a
266 focused electron beam in a high-vacuum environment using a SUPRA 55 CARL ZEISS
267 (Germany) microscope, which offers a resolution of 200 Å and a magnification range of 35 to
268 10,000x.

269 **2.6.5 TGA (Thermogravimetric Analysis)**

270 The Surface Temperature Meter (SDT) Q600 V20.9 Build 20 was used for
271 thermogravimetric analysis (TGA) and differential scanning calorimetry (DSC) of the nano-
272 encapsule in the temperature range of 37° C to 700 °C using a heating rate of 7 C/min in a
273 nitrogen.

274 **2.7 Antioxidant activity**

275 **2.7.1 DPPH free radical scavenging activity**

276 The DPPH radical scavenging assay, as outlined by Blois (1958), and the modified
277 method by Rahman et al. (2015) were used to evaluate the CT-CS-LA-NC methanolic extract's
278 and the standard's capacity to scavenge free radicals. A 0.1 mM DPPH in methanol solution
279 was made, and 100 µl of this solution was added with the CT-CS-LA-NC methanolic extract
280 at several concentrations (20–100 µg/ml). In methanol solution, DPPH appears violet/purple
281 but fades to yellow when antioxidants are present. At 517 nm, the absorbance was measured.
282 Using the following formula, the percentage of DPPH radical scavenging activity was
283 determined:

$$284 \quad \% \text{ DPPH free radical scavenging activity} = [(A_0 - A_1) / (A_0)]$$

285 where A_0 is the absorbance of the control, and A_1 is the absorbance of the extractives/standard.
286 Then the % of inhibition was plotted against concentration, and from the graph, IC_{50} was
287 calculated using linear regression. The experiment was repeated three times at each
288 concentration.



289 2.8 Antibacterial activity

290 Antibacterial activity of the nano capsule was tested against *Bacillus subtilis* (ATCC
291 6051) and *Escherichia coli* (ATCC 25922) adopting a well diffusion assay. All the experiments
292 were carried out with free *L. acidophilus*, nano-encapsulated *L. acidophilus*, and secretors of
293 free *L. acidophilus* and nano-encapsulated *L. acidophilus* separately. Inocula of respective
294 treatments were prepared in MRS broth incubated at 37°C for 18 hours. The secretory product
295 of *L. acidophilus* was obtained from the culture supernatant of the respective treatment group
296 (inoculated MRS broth centrifuged at 8000 RPM for 10 mins; the collected supernatant was
297 syringe filtered and used as the source for antibacterial activity. Inocula of the respective
298 bacterial cultures prepared in MRS broth were uniformly spread on the sterile MRS agar media.
299 Wells were made on the swabbed agar using a sterile gel puncture (8 mm). 100 µl of viable
300 inocula of *L. acidophilus* thus prepared was added to the wells. For 24 hours, the seeded plates
301 were incubated at 37°C [29]. The plates were examined for zones of inhibition following the
302 incubation period.

303 2.9 Evaluation of Acid Tolerance

304 The modified acid tolerance test was performed as described previously by Ehrmann et
305 al. (2002). Acid stress condition was created by adjusting the pH of the MRS broth to 2.5 using
306 1N HCl in addition. The inoculum thus prepared was added to 100 ml of sterile MRS broth in
307 various conical flasks at concentrations (v/v) ranging from 0.5 ml to 2.5 ml, respectively, and
308 incubated at 37°C under shaking conditions. Additionally, the CT-CS-LA-NC was suspended
309 in the MRS broth at concentrations (w/v) varying from 0.5 g to 2.5g and incubated for 48 hours.
310 These treatment groups were observed and compared against a control group. The turbidity of
311 the culture media was monitored at several time intervals (12 hours, 24 hours, and 36 hours).
312 After the incubation period, the optical densities (OD 570 nm) were recorded at 12-hour
313 intervals for 48 hours. The negative control, which was only the media, showed no growth.



314 The same procedure was repeated for all the treatment and control groups under the same
315 experimental conditions, respectively. All tests were carried out in triplicate.

316 **2.10 Evaluation of Bile tolerance**

317 A previously adapted technique by Akmal et al. (2022) was used to assess bile
318 tolerance. The simulated bile conditions were prepared by adding 0.3 g in 100 mL (0.3% w/v)
319 of MRS broth and using a 1 M sodium hydroxide solution to adjust the pH to 7.5. After
320 preparation, 100 mL of sterile MRS broth in various conical flasks were filled with the
321 inoculum at concentrations ranging from 0.5% (v/v) to 2.5% (v/v), respectively, and shaken
322 while being incubated at 37°C. After being dissolved in the MRS broth at concentrations
323 varying from 0.5% (w/v) to 2.5% (w/v), the CT-CS-LA-NC was incubated for 36 hours. These
324 treatment groups were observed and contrasted with the control group. There was no growth
325 in the negative control, which consisted solely of the media. Followed by a spectrophotometer
326 was used to measure the track bacterial growth at 560 nm. Every experiment was run in
327 triplicate.

328 **2.10 Storage stability**

329 The stability and storage conditions of the free probiotic and CT-CS-LC-NC were
330 comparatively evaluated over 28 days adapted method from Thinkohkaew et al. (2024). Both
331 the encapsulated alginate beads and the free probiotic cell suspension were stored in sterile
332 conical tubes containing 0.5% sterile sodium chloride (NaCl) solution at 4°C. The viability of
333 the probiotics in the free suspension and the beads was assessed at different time periods,
334 including 7, 14, 21, and 28 days. The encapsulated samples were dissolved in NaCl to release
335 cells. Followed by Serial dilutions and dot-plating method the viable cell count was measured
336 on the MRS agar plates. The plates were incubated at 37°C for 48 hours before colony-forming
337 units (CFU) were counted. The survival rate for each sample at each time point was then



338 determined and compared to the initial viable cell count to determine the probiotic viability
339 under refrigerated conditions.

340 **2.11 Ecotoxicity assessment of CT-CS-LA-NC**

341 Ecotoxic effect of fabricated nano-encapsule was determined by measuring phytotoxic
342 effect and soil parameters.

343 **2.11.1 Seed germination exposure**

344 The *Vigna mungo* seeds were first rinsed thoroughly in deionized water and further
345 surface sterilized with a 70% ethanol solution to reduce microbial contamination. For
346 treatment, seeds were immersed for 24 hours in a homogenized blend of CT-CS-LA-NC. This
347 essential soaking procedure was carried out in darkness at ambient temperature to emulate
348 standard pre-sowing treatment conditions while regulating light conditions. 16 *Vigna mungo*
349 seeds were carefully dried after treatment, and the germination assay was started by transferring
350 them to Petri dishes with a filter paper. After that, they were kept at room temperature in a dark
351 environment. Distilled water was sprayed twice a day in a fine mist with a 12-hour gap between
352 applications to maintain ideal moisture levels adapted from the method followed by Abbas et
353 al. (2024). All of the tests were done in triplicate.

354 **2.11.2 SDS-PAGE (Sodium Dodecyl Sulfate-Polyacrylamide Gel Electrophoresis)**

355 According to Fling and Gregerson (1986), SDS-PAGE was used to assess the
356 differences in the protein profile of plant tissue taken from the respective treatment and control
357 group. For extraction of proteins, black gram seeds were ground to fine powder. Sample buffer
358 (1.5 M Tris-HCl, 1% SDS, 30% glycerol and 2% β -mercapto ethanol, pH 6.8) 1:1 was mixed
359 with protein extracts. Protein movement in the gel was observed by adding Bromophenol Blue
360 (BPB) as a tracking dye to the sample buffer. The control and treated samples' crude protein
361 extracts were dissolved in sodium phosphate buffer (pH 7.5) and centrifuged for three minutes
362 at 10,000 rpm. Soluble proteins were separated using stacking and linear gradient acrylamide



363 separating gels at a constant current until the tracking dye reached the separating gel's edge
364 Coomassie Brilliant Blue R-250 (CBBR) staining was applied to the gels. 0.05 M tris-glycine
365 buffer was used for the electrophoresis, which was carried out at 10°C (pH 8.3) until the sample
366 bands crossed the stacking layer. The protein bands were visualized.

367 **2.12 In-silico docking**

368 The 3D structures of the proteins were obtained from the RCSB PDB database
369 (<http://www.rcsb.org/pdb>) using the following PDB IDs: 7K41, 8AE1. The ligand molecules
370 Anthocyanin (PubChem CID: 154824275), Chitosan (PubChem CID: 441477), and Lactic
371 Acid (PubChem CID: 612) were obtained from the PubChem website
372 (<http://pubchem.ncbi.nlm.nih.gov>). The target proteins' optimal protein-ligand interaction sites
373 were found using CB Dock software, which also computes the target proteins' size and shape
374 using a curvature-based cavity identification technique and performs docking using Auto Dock
375 Vina software. Based on Vina scores, CB-Dock evaluates the binding modes and provides an
376 interactive three-dimensional model of them [35].

377 **2.13. Statistical analysis**

378 All data were obtained from at least in duplicate experiments. The results were
379 compared using one-way analysis of variance (ANOVA) followed by Duncan's post-hoc
380 (Prism Software version 5.0). Results were considered significant when $p < 0.05$.

381 **3. Result and Discussion**

382 **3.1 Isolation and identification of *L. acidophilus***

383 The probiotic strain *L. acidophilus* used in this study is isolated from the curd by a
384 culture-dependent method. The serially diluted curd sample was spread plated on sterile MRS
385 agar followed by incubation under optimum conditions (Identification of the isolate was done
386 by morphological and biochemical properties shown in Table.1). The *L. acidophilus* was
387 isolated from curd. The selected bacterial strain was identified by morphological, and



388 biochemical characterized as *L. acidophilus*. Morphologically the single colonies were circular
389 and creamy white. The bacteria were Gram-positive rods and cocci-shaped, were further
390 observed under phase contrast microscope as shown in the Fig.S1. This study revealed gram-
391 positive, non-spore-forming rods showing negative result (red colour), All the isolated strains
392 were found to be catalase-negative (no bubbles formation), and indole test-negative bacteria
393 This is in agreement with the study conducted by Rozos et al. (2018). Thus, the results obtained
394 coincided with *L. acidophilus* strain characteristics.

395 3.1.1 16SrRNA Sequencing and Phylogenetic Analysis

396 After the confirmation, the isolated *L. acidophilus* was stored on MRS agar slant for
397 further studies. Inoculating the *L. acidophilus* for the nano-encapsule was prepared in sterile
398 MRS broth. *L. acidophilus* was seeded, and the broth was centrifuged, followed by collecting
399 the cell pellets. Cells were washed with sterile PBS, and the washed cells were used as the
400 source of inoculum. Final yield of the inoculate was found to be 1.0% w/v; the healthy
401 inoculum thus prepared was used for further studies.

402 The 16SrRNA gene sequence of isolated strains showed 96% similarity to *L.*
403 *acidophilus*. All isolated strains corresponding to *Lactobacillus* was considered to be the best
404 match based on top hit similarity [37]. The sequence has been deposited in the NCBI GenBank
405 database under accession number PX470079. The phylogenetic trees were designed in the
406 bootstrap neighbor-joining (NJ) method Fig. S2 based on 16SrRNA gene sequencing.

407 3.2 Preparation of *C. ternatea* extract coated chitosan-*L. acidophilus* Nano encapsule (CT- 408 CS-LA-NC)

409 *C. ternatea* extract-coated chitosan-*L. acidophilus* nano-encapsulate was prepared by
410 the simple in-situ principle of *C. ternatea*, which was readily extracted in distilled water at
411 ambient conditions, and the final yield of the metabolite was found to be 1.029 g/L. The
412 extracted metabolite was stored in screw cap vials and used for further studies. Phytochemical



413 screening of *C. ternatea* leaves indicated the presence of active components such as alkaloids,
414 flavonoids, tannins, phenols, and saponins, with steroids being absent shown in Table. 2. In a
415 related study Neda, et al. (2013) detailed the phytochemical compounds and nutritional
416 composition found in *C. ternatea* flowers.

417 Simple insitu dispersion method was employed for the preparation of nanoencapsule.
418 Opaque probiotic nano capsules with a sphere-like structure (Fig.1) and highly stable
419 characteristics were fabricated using *C. ternatea* extract, chitosan polymer, and *L. acidophilus*.
420 Synthesized CT-CS-LA-NC was characterised by techniques like Scanning Electron
421 Microscope, Fourier transform infrared spectroscopy, Thermogravimetric analysis. Among the
422 various substances, chitosan is an important polymer used for the encapsulation of probiotic-
423 stabilised nano-encapsulates, revealing enhanced biological activities. Chitosan improves
424 solubility, stability and resistance to degradation, which offers controlled drug delivery to
425 specific sites and has enhanced antimicrobial properties [39,40]

426 3.3 Encapsulation efficiency of CT-CS-LA-NC

427 The encapsulation efficiency (EE) of the CT-CS-LA-NC beads was found to be 98.43%
428 (Fig. S3). The CT-CS-LA-NC coating material's significant efficacy in preserving the probiotic
429 cells during the encapsulation process is due its high efficiency. The results of the present study
430 agreed with Afzaal et al. (2020) who reported sodium alginate microbeads encapsulate
431 probiotics 98% more effectively than carrageen. The alginate matrix entraps more cells than
432 the other material, but both materials entrap the necessary number of cells. Probiotic survival
433 is increased by encapsulation with alginate and whey protein, suggesting that efficient probiotic
434 consumption is necessary for colonization in colon.

435 3.4 Characterization techniques

436 3.4.1 Poly dispersive index



437 The Dynamic Light Scattering (DLS) analysis confirmed the formation of the CT-CS-
438 LA-NC composite within the targeted nanometer size range. The Z-Average size measured was
439 162 nm, categorizing the overall distribution within the sub-micron scale, which is optimal for
440 targeted delivery. The distribution exhibited a notable and significant peak, validating the
441 synthesis of chitosan nano encapsules with a mean diameter of 91.1 nm (Fig. S4). The results
442 indicate effective encapsulation of *L. acidophilus* within a stable, nano-structured delivery
443 system.

444 3.4.2 Zeta potential

445 According to the surface zeta potential of CT-CS-LA-NC, which was measured to be
446 -54.7 ± 0.32 mV, it can be concluded that the nanoparticles in the dispersant (water) exhibit a
447 high degree of electrostatic stability (Fig.S5). This analysis is essential for interpreting the
448 colloidal behaviour of Chitosan NPS material. The significant negative charge indicates that
449 the particles repel each other, consequently minimizing aggregation. Stability in chitosan
450 formulations may be due to coating or loading anionic components, such as phenolics from *C.*
451 *ternatea* extract or other stabilizing excipients, resulting in a stable Nano-encapsule rather than
452 a cationic core. The research conducted by Weng et al. (2022) reported that the surface zeta
453 potential of *L. acidophilus* cell envelope LA/TCS@PLGA-NPs was -21.3 ± 0.46 mV. The
454 observed increase in zeta potential indicates a charge screening effect attributed to the coated
455 envelope. A study conducted by Barrera-Necha et al. (2018) demonstrated that chitosan
456 nanoparticles, when combined with botanical extracts, exhibited a Zeta potential value of -43.8
457 mV.

458 3.4.1 Scanning Electron Microscope (SEM)

459 This SEM image reveals significant details about the surface morphology of the nano-
460 encapsulated composite of plant extract (*Clitoria ternatea*), probiotic (*Lactobacillus*), and



461 chitosan. The surface topology of the CT-CS-LA-NC nano-encapsules, as shown in Fig 2, was
462 analysed using SEM. With its densely packed, complex surface topology, the SEM micrograph
463 displays irregular particles with consistent shape homogeneity, indicating good nanocomposite
464 encapsulation and stability. The relatively smooth surface morphology suggests a uniform
465 distribution of the *Clitoria ternatea* extract and probiotics within the chitosan matrix, indicating
466 an efficient encapsulation process and strong integration (Fig 2). According to the SEM image,
467 the average size of synthesized nano-encapsule is 5 μm and the image suggests that the
468 structures found are either uniform or non-uniform and fall within the nanometre range [44].
469 Based on this SEM analysis, the nanoencapsulation process appears to have successfully
470 formed composite structures, suggesting efficient interaction between the chitosan, probiotic,
471 and plant extract which could influence the release dynamics in pharmacological applications
472 [45].

473 3.4.2 Fourier transform infrared spectroscopy (FTIR)

474 The vibrational characteristics of the Chitosan-Alginate Nanoencapsule (CS-NC)
475 control shows a broad and intense peak at 3344.49 cm^{-1} , reflects the merged stretching
476 vibrations of hydroxyl (O-H) and amine (N-H) groups inherent to the chitosan framework. The
477 peaks in the fingerprint region further confirm the polymer's structure. A strong band at
478 1587.15 cm^{-1} is linked to the N-H bending, and the characteristic absorption bands at 1424.25
479 cm^{-1} and 1330.35 cm^{-1} are linked to the C-H bending and C-N stretching, respectively. The
480 band at 1052.50 cm^{-1} indicates C-O-C glycosidic linkage and C-O stretching, confirming
481 chitosan's polysaccharide composition and structure.

482 The FTIR spectroscopy results of the synthesized Chitosan-Probiotic-*Clitoria ternatea*-
483 Nano encapsule (CT-CS-LA-NC) revealed absorption peaks across a range of 720 cm^{-1} to 3350
484 cm^{-1} , signifying molecular interactions and the presence of various functional groups (Fig. 3).
485 The peak at 3350 cm^{-1} might be related to O-H stretching, which indicates that hydroxyl groups



486 are present. Chitosan mostly consists of N-H and O-H stretching, amide bands, C-O-C
487 stretching, and C-H stretching, among several other peaks [46,47]. Broad absorption peaks at
488 2922cm^{-1} and 2855 cm^{-1} suggest C=O carboxyl stretching and typical C-H stretching in
489 alkanes, respectively. A sharp peak at 1582 cm^{-1} could correspond to C=C stretching vibrations
490 in aromatic compounds [48]. The distinct peaks at 1421 cm^{-1} and 1326 cm^{-1} are often
491 indicative of C-C stretching (Kumar & Mohideen, 2024). Additionally, the absorption at
492 1018.44 cm^{-1} might represent C-N stretching vibrations found in ethers or alcohols, signifying
493 the presence of aliphatic amines [49]. Lastly, the peak at 721 cm^{-1} is commonly associated
494 with C-H rocking modes, further confirming the molecular characteristics of the nano
495 encapsulated structure. Senthil Kumar et al. (2024) has reported that this is due to glycosidic
496 linkages in chitosan, polysaccharides, and the bacterial cell wall of *Lactobacillus fermentum*.
497 Chitosan (CS) is the reference peak, and shifts in existing peaks can be attributed to interactions
498 between compounds. This can be explained by the glycosidic bonds present in polysaccharides,
499 present in chitosan as well as the bacterial cell wall of *Lactobacillus fermentum* [50]. With
500 chitosan (CS) as a reference peak, we can confirm the presence of chitosan in the synthesised
501 NPs and mild shifts in existing peaks could be linked to interactions between the bacterial
502 components [51]. The FTIR spectra of the CS-NC (Fig. 3 A). control and the CT-CS-LA-NC
503 (Fig. 3 B) show significant structural modifications. The CT-CS-LA-NC spectrum reveals the
504 two bands at 2922 cm^{-1} and 2855 cm^{-1} , indicating the presence of organic compounds such
505 lipids, proteins from *L. acidophilus*, and organic acids from *C. ternatea*. These peaks are absent
506 in the pure chitosan control. The shift in the N-H bending/Amide II peak from 1587.15 cm^{-1}
507 in the control to 1581.63 cm^{-1} in the formed sample confirms the encapsulation of the plant
508 extract. The most significant change is the shift of the characteristic chitosan C-O/C-N
509 stretching peak from 1052.50 cm^{-1} to 1018.44 cm^{-1} . This shift suggests that the encapsulated

View Article Online
DOI: 10.1039/D3FB00833F



510 components and chitosan have strong molecular interactions, which confirms the successful
511 chemical integration and stabilization of the nanocomposite.

512 3.4.3 Thermogravimetric analysis

513 The thermal stability of the synthesised nano-encapsule (CT-CS-LA-NC) was
514 determined by thermogravimetric analysis, which measures weight loss in relation to rising
515 temperature [52]. The weight of the nano-encapsule gradually decreases as the temperature
516 rises when the sample is heated from 20° C to 200° C at intervals of 10° C.

517 (Fig.4). The sample weighed 2.2590 mg initially, and as the temperature increased, the mass
518 changed. At 49.85°C, a slight weight loss of 0.1010% was noted during the initial
519 decomposition stage. This implies the elimination of any remaining moisture or volatile
520 components, which is common for materials based on chitosan, according to the Zhang et al.
521 (2021) study. This significant loss suggests the breakdown of polymeric structures, such as
522 chitosan and probiotic encapsulation materials, due to thermal degradation. The weight
523 percentage dropped to 0.0618% in the second decomposition stage at 100.26°C indicating
524 further water loss or slight degradation of low-molecular-weight compounds. At end of the
525 experiment, a final retained weight of 10.68% was recorded, indicating a total weight loss of
526 0.2412 mg. The results obtained by Hong et al (2007) confirm the existence of several thermal
527 degradation phases and indicate that nanoencapsulation improves thermal stability by
528 postponing degradation relative to pure chitosan.

529 3.5 Antibacterial activity

530 Antibacterial activity was tested against *E. coli* and *B. subtilis* using a well-diffusion
531 assay. The assay was performed with viable inocula of the respective *L. acidophilus* treatment
532 groups, including their secretory products. The results showed that all treatments inhibited the
533 growth of both bacterial strains. The nano-encapsulated *L. acidophilus* and its secretory product
534 exhibited the largest zones of inhibition for *Escherichia coli*, measuring 14.2 ± 0.26 cm and



535 14.3 ± 0.27 mm, respectively. The zone of inhibition formed by the secretory product of the
536 free *L. acidophilus* was 13.1 ± 0.17 cm, whereas the smallest zone was established by the free
537 *L. acidophilus* itself, measuring 12 ± 0.19 mm for *Bacillus subtilis* as shown in Table.3. The
538 nano-encapsulated *L. acidophilus* and its secretory product was similarly quite effective
539 which exhibited a zone of inhibition of 15.1 ± 0.24 mm and 14.4 ± 0.32 mm. The inhibition of
540 the free *L. acidophilus* and its secretory product was similar, with zones of 13 ± 0.19 mm and
541 13.4 ± 0.21 mm, respectively. Similar to the viable inocula, the secretory products from both
542 free and encapsulated formulations showed growth inhibition. These findings are consistent
543 with Soltani et al. (2022) who reported that the most significant growth inhibition zones were
544 associated with the extracts of *L. acidophilus* (16 mm) and *L. casei* (15 mm) strains. The
545 secretome of both *Lactobacillus* strains exhibited a greater growth inhibition zone.

546 3.6 Antioxidant Activity

547 3.6.1 DPPH free radical scavenging activity

548 DPPH is a stable free radical that changes color to purple when dissolved in methanol.
549 The reaction between free radicals and antioxidants changes their colour from purple to yellow,
550 which in turn changes their properties. The concentration of the assessed free *L. acidophilus*,
551 CT-CS-LA-NC, and ascorbic acid varied between 200 and 1000 µg/mL. The antioxidant
552 activity test with DPPH was compared to standard concentrations (ascorbic acid) using a linear
553 regression analysis to assess efficiency and consistency. The DPPH activity graph shows a
554 concentration-dependent rise in free radical scavenging for all three tested materials, with the
555 nanocomposite CT-CS-LA-NC exhibiting the highest antioxidant efficacy across all
556 concentration ranges. At the maximum concentration of 1000 µg/mL, the CT-CS-LA-NC
557 sample reaches 48.2 ± 1.32% inhibition, showing an increase over the free *L. acidophilus* cells
558 (16.75±0.98%) (Fig.5). This significant enhancement in activity suggests a synergistic effect
559 resulting from the incorporation of *Clitoria ternatea* (CT) into the CT-CS-LA (NC), indicating



560 that the nanocomposite preparation exhibits high antioxidant delivery system compared to the
561 standard and the free probiotic cells. The IC_{50} of CT-CS-LA-NC was determined to be 28.04
562 $\mu\text{g/mL}$, whereas the IC_{50} of free *L. acidophilus* was 3.22 $\mu\text{g/mL}$, and both were compared to
563 the standard ascorbic acid concentration ($IC_{50} = 1.61 \mu\text{g/mL}$). The antioxidant activity of *C.*
564 *ternatea* flower solvent or water extracts has been measured previously by Jeyaraj et al.,
565 (2022), and the anthocyanin-rich a proportion has more efficacy than the crude extracts, with
566 IC_{50} values of 1.24 $\mu\text{g/mL}$ respectively. *C. ternatea* and chitosan both have natural antioxidant
567 and antibacterial properties. Flavonoids present in *C. ternatea* also have a wide range of
568 antimicrobial effects. Together, these three components exhibit a strong synergistic resistance
569 [56]

570 3.7 Viability of free *L. acidophilus* and CT-CS-LA-NC in acidic condition

571 Probiotic bacteria are typically delivered in food systems and must be acid tolerant to
572 survive in the human gastrointestinal tract. The average time from entry to release from the
573 stomach is ninety minutes, though this can vary depending on other digestive processes (Ding
574 & Shah, 2009). Encapsulation improves the survival of probiotic bacteria by providing a
575 protective barrier against harsh environmental conditions, such as the stomach's low pH. This
576 barrier protects the cell membrane and cell wall from being destroyed right away, allowing the
577 bacteria to travel through the gastric environment and into the intestine [57].

578 In this acid tolerance study, the survival of free *Lactobacillus acidophilus* and nano-
579 encapsulated CT-CS-LA-NC was assessed under simulated gastric conditions at pH 2.5 and
580 pH 3.5 over 12, 24, and 36 hours is shown in Table.S1 & Table.S2. The concentration of free
581 *L. acidophilus* and CT-CS-LA-NC was varied from 0.5 mL to 2.5 mL. Initially at pH of 2.5,
582 the acid resistance of free *L. acidophilus* was moderate over 12 hours, with survival rates
583 varying from 12.08 ± 0.10 to 37.80 ± 0.21 . The nano-encapsulated CT-CS-LA-NC showed a
584 similar survival rate, ranging from 1.07 ± 0.12 to 36.49 ± 0.34 . Free cells showed better



585 viability 4.51 ± 0.21 to 25.12 ± 0.16 than the nano encapsulated cells 2.58 ± 0.15 to $23.26 \pm$
586 0.16 after 24 hours of acid exposure. The lower total viable count compared to the free cells
587 may result from the probiotic's gradual and prolonged release from the encapsulation.
588 However, the most significant difference was seen after 36 hours (Fig.6). Encapsulated cells
589 showed highly significant survivability rate of 60.93 ± 0.68 at 2.5 ml. In contrast, the survival
590 of free *L. acidophilus* peaked at only 45 ± 0.13 .

591 At pH 3.5, CT-CS-LA-NC maintained similar vitality ranging from 1.93 ± 0.18 to 50.23
592 ± 0.43 after 12 hours of exposure whereas free *L. acidophilus* also showed, similar vitality
593 (5.47 ± 0.24 to 36.68 ± 0.26). Free cells survivability decreased at 24 hours (4.85 ± 0.02 to 9.80
594 ± 0.08). After 36 hours, CT-CS-LA-NC showed 76.46 ± 0.60 (2 ml), exceeding free cells
595 (65.42 ± 0.73) and exhibiting enhanced acid tolerance. The survivability of CT-CS-LA-NC
596 was greatly improved confirming the enhanced acid tolerance (60.93 ± 0.68) at 2.5 ml after 36
597 hours, compared to 45 ± 0.13 for free *L. acidophilus*, indicating the high efficiency of the
598 encapsulated *L. acidophilus* (Fig.7).

599 These results correspond with prior research. Varela-Pérez et al. (2022) indicated that
600 nanoencapsulation improves probiotic survival in acidic conditions. Arratia-Quijada et al.
601 (2024) examined persistent acid tolerance in encapsulated strains. Argyri et al. (2012)
602 highlighted that resistance to low pH is specific to strains, employing pH 2.5 to identify acid-
603 tolerant *Lactobacilli*. The results indicate the survival rate at different concentrations and time
604 intervals, showing CT-CS-LA-NC's efficiency in preserving probiotic viability under
605 simulated gastrointestinal circumstances. Chitosan acts as a prebiotic, providing nourishment
606 for probiotics such as *L. acidophilus* in the large intestine [61]. The synbiotic effect - the
607 combination of a probiotic and a prebiotic—substantially enhances the colonization and
608 therapeutic advantages of the encapsulated bacteria. The synergistic relationship between the
609 components of the product enhances probiotic viability, stability, and therapeutic potential,



610 providing a robust protective effect against gut pathogens, ensuring successful delivery of *L.*
611 *acidophilus* [62].

612 3.8 Viability of free *L. acidophilus* and CT-CS-LA-NC in bile conditions

613 The survival rates of both free and nano-encapsulated *L. acidophilus* (CT-CS-LA-NC)
614 under two pH values (2.5 and 3.5) over 12, 24, and 36 hours were investigated in this bile
615 tolerance study is shown in Table.S3. At a low concentration of 0.5 ml, the tolerance of the
616 free *L. acidophilus* cells was significantly higher than that of the nano-encapsulated cells (5.39
617 ± 0.13). This implies that the encapsulation might slowly dissolve or activate. However, the
618 nano-encapsulated CT-CS-LA-NC cells showed a noticeably higher tolerance when the
619 concentrations were raised to a higher level (between 1 and 2.5 mL). The CT-CS-LA-NC
620 maximum tolerance at 2.5 ml was 35.24 ± 0.3 , greater than the free cell maximum tolerance of
621 32.41 ± 0.12 .

622 After 24 hours of exposure, the slow-release profile of CT-CS-LA-NC was noticeably
623 superior to that of free *L. acidophilus*. Across a range of nanoencapsulation concentrations (0.5
624 ml to 2.5 ml), CT-CS-LA-NC demonstrated significantly higher survival rates. CT-CS-LA-NC
625 exhibited a survival rate of 19.25 ± 0.15 at the lowest concentration of 0.5 ml, whereas free
626 cells only showed an 11.56 ± 0.21 survival rate (Fig.8). As exposure duration increases, nano-
627 encapsulation significantly enhances protection against bile tolerance, as shown by its
628 consistent performance across all of the various concentrations that were assessed. After 36
629 hours, the highest survivability rates were found in encapsulated cells. At all concentrations,
630 CT-CS-LA-NC's tolerance was significantly greater than that of free *L. acidophilus*. The
631 survival of free *L. acidophilus* was only 21.29 ± 0.13 , while the encapsulated cells
632 demonstrated a survivability of 39.46 ± 0.68 at 2.5 ml. This extremely significant difference
633 highlights the high effectiveness of the encapsulated *L. acidophilus* (CT-CS-LA-NC) in



634 resisting the harsh environment of bile acids, particularly at higher concentrations and for
635 longer periods of time.

636 **3.6 Ecotoxicity assessment of CT-CS-LA-NC**

637 **3.6.1 Seed germination assay**

638 *Vigna mungo* treated with 5% of CT-CS-LA-NC showed a promotion in plant growth.
639 Results indicate that CT-CS-LA-NC has not shown any toxic effect on seedling emergence.
640 CT-CS-LA-NC-treated seeds showed 96% of the seedling's emergence in *Vigna mungo* (Fig.
641 9). The control group showed a 100% growth rate. These findings suggest that using CT-CS-
642 LA-NC enhances seedling emergence. The difference of only 2.19% between the treatment and
643 control groups suggests that the nano-encapsules had no significant inhibitory effect on seed
644 viability. The control set showed $98 \pm 0.21\%$ of germination. The GP value of 96.81% ($P \leq$
645 0.05) in the treatment set indicates that nearly all of the treated seeds germinated, supporting
646 the conclusion that the CT-CS-LA NC treatment did not inhibit or interfere with the biological
647 processes involved in seedling germination.

648 **3.6.2 Protein profiling study using SDS-PAGE**

649 SDS-PAGE analysis of protein extracted from *Vigna mungo* provided insights into the
650 impact of CT-CS-LA-NC treatment on protein expression (Fig.10). Molecular weight
651 estimation using reference markers (245 kDa to 17 kDa) revealed 15 distinct protein bands,
652 with fainter bands between 35 kDa and 25 kDa suggesting potential regulatory protein
653 modifications. According to the study by Torio et al. (2011) the major storage protein, 8S α
654 globulin, identified as a trimer of subunits at 49 kDa, was prominently expressed in lanes 2, 3,
655 and 5, as well as in the control. Comparisons between control and treated groups demonstrated
656 shifts in protein profiles, highlighting the effects of CT-CS-LA-NC interaction [64]. SDS-
657 PAGE effectively facilitated molecular weight characterization and regulatory insights into
658 protein expression in *Vigna mungo*.



659 3.7 Storage stability

View Article Online
DOI: 10.1039/D5FB00833F

660 The probiotic cells encased in an encapsulating matrix must endure severe conditions,
661 including external factors and the gastrointestinal tract, while also preserving their viability
662 during storage. The storage temperature has a major impact on the viability of the cells during
663 the storage time. This study involved the storage of free *L. acidophilus* cells and encapsulated
664 cells at a refrigerated temperature of 4 °C. Fig.11 depicts the storage stability of free *L.*
665 *acidophilus* and CT-CS-LA-NC probiotics when stored at refrigeration temperature of 4°C for
666 a duration of 28 days. The viability of the free cells showed rapid decline, in the survival rate
667 decreasing from an initial 7.98 to 7.8 log₁₀ CFU/ mL by the end of 28-days. However, the CT-
668 CS-LA-NC encapsulated cells also had similar higher survival rate, retaining 7.84 log₁₀ CFU/
669 mL viability after 7 days and maintaining more than half of their initial population till 14 days
670 after 28 days. Probiotic viability and storage durability are enhanced by the steady and gradual
671 release of cells from the coating material, chitosan biopolymer, which traps *L. acidophilus*
672 inside the alginate. Fareez et al. (2014) reported that while decreasing viability loss at 75 and
673 90°C, Alg-XG-Ch increased the storage durability of *L. plantarum* LAB12 at 4°C and *L.*
674 *plantarum* LAB12, combined in Alg-XG-Ch, might be used as a new functional food ingredient
675 with health benefits.

676 3.8 In-silico docking

677 In the present study, the docking analysis focused on identifying the molecular
678 interactions between two proteins associated with probiotics, O-GlcNAcase (7K41) and S-
679 layer associated protein (SlpA) (8AE1), along with three significant compounds from the
680 nanoencapsulated system, such as anthocyanin, lactic acid, and chitosan (Fig.12). Anthocyanin
681 has a high binding affinity for O-GlcNAcase (7K41) and SlpA (8AE1), with interaction scores
682 of -9.4 kcal/mol and -9.6 kcal/mol, respectively. These interaction scores show that
683 Anthocyanin forms stable complexes with proteins, indicating its potential to impact their



684 functions, which consistent with previous studies on its bioactivity, which is associated with
685 its ability to interact with proteins. According to the study by Hidalgo et al. (2012) which
686 contributes to the preservation of gastrointestinal health by modulating the microbial
687 composition of the gut and providing antioxidant activity in the large intestine. Chitosan
688 exhibited significant interaction scores of -5.2 kcal/mol for O-GlcNAcase and -5.4 kcal/mol
689 for SlpA, show in Table.4 indicates the distinct binding sites (534 for 7K41 and 2163 for 8AE1)
690 on each protein. Its interaction with SlpA, a key component of the bacterial cell wall, supports
691 its role in protecting the cell membrane. Likewise, Lactic acid also had notable interaction
692 scores of -4.1 kcal/mol (7K41) and -3.8 kcal/mol (8AE1). These in silico findings explain the
693 nano-encapsulated system's synergistic effects and emphasize the molecular interactions
694 between anthocyanin, chitosan, and lactic acid.

695 4. Conclusion

696 The study successfully demonstrates the nanoencapsulation of *Lactobacillus*
697 *acidophilus* using chitosan and *Clitoria ternatea* extract (CT-CS-LA-NC). The effective
698 encapsulation of *Lactobacillus acidophilus* using this approach presents new possibilities for
699 its use as a biopreservative in functional foods, drinks, and nutraceuticals. This method's
700 effective encapsulation of *Lactobacillus acidophilus* creates potential opportunities for its use
701 as a biopreservative in nutraceuticals, functional foods, and drinks. Nanoencapsules with
702 improved thermal and acid stability would facilitate the development of novel probiotic-
703 enriched products, such as juices, food products, and dietary supplements, which are
704 traditionally difficult to formulate with probiotics. It may also be able to prolong the shelf life
705 of perishable goods, eliminating the need for artificial preservatives, given its proven
706 antibacterial qualities against common food pathogens like *B. subtilis* and *E. coli*. CT-CS-LA-
707 NC provides a versatile and sustainable solution that offers both functional health advantages



708 and enhanced product stability in response to the growing consumer demand for natural
 709 products.

710 **Declaration**

711 Ethical Approval

712 Not applicable

713 Consent to Participate

714 Not applicable

715 Consent to Publish

716 We consent to publish in this journal

717 Authors Contributions

718 M.Lavanya- Data curation, formal analysis, investigation, methodology, software, original
 719 manuscript writing

720 S.Karthick Raja Namasivayam- Conceptualization, supervision, investigation, manuscript
 721 review & editing

722 Funding

723 The work has not received any funds

724 Competing Interests

725 We declare no conflict of interest

726 Availability of data and materials

727 The data will be made available on request from the authors

728 **Reference**

- 729 1. S. K. Amit, Md. M. Uddin, R. Rahman, S. M. R. Islam and M. S. Khan, *Agriculture &*
 730 *Food Security*, 2017, **6**.
- 731 2. Mc. Martínez-Ballesta, Á. Gil-Izquierdo, C. García-Viguera and R. Domínguez-Perles, *Foods*,
 732 2018, **7**, 72.



- 733 3. T. Didari, S. Solki, S. Mozaffari, S. Nikfar and M. Abdollahi, *Expert Opinion on Drug* View Article Online
DOI: 10.1089/D5FB00833F
734 *Safety*, 2014, **13**, 227–239.
- 735 4. R. R. Watson and V. R. Preedy, *Probiotics, prebiotics, and synbiotics: Bioactive Foods in*
736 *Health Promotion*, Academic Press, 2015.
- 737 5. S. Fijan, *International Journal of Environmental Research and Public Health*, 2014, **11**,
738 4745–4767.
- 739 6. P. A. Mackowiak, *Frontiers in Public Health*, 2013, **1**.
- 740 7. A. Latif, A. Shehzad, S. Niazi, A. Zahid, W. Ashraf, M. W. Iqbal, A. Rehman, T. Riaz, R.
741 M. Aadil, I. M. Khan, F. Özogul, J. M. Rocha, T. Esatbeyoglu and S. A. Korma,
742 *Frontiers in Microbiology*, 2023, **14**, 1216674.
- 743 8. K. Prajapati, K. Bisani, H. Prajapati, S. Prajapati, D. Agrawal, S. Singh, M. Saraf and D.
744 Goswami, *Systems Microbiology and Biomanufacturing*, 2023, **4**, 386–406.
- 745 9. M. Bernatek, H. Sommermeyer, A. Wojtyła, J. Piątek and S. Lachowicz-Wisniewska,
746 *Journal of Health Inequalities*, 2023, **9**, 194–200.
- 747 10. M. L. Marco and S. Tachon, *Current Opinion in Biotechnology*, 2012, **24**, 207–213.
- 748 11. A. Pugazhendhi, M. A. Alshehri, S. Kandasamy, P. K. Sarangi and A. Sharma, *Food*
749 *Chemistry*, 2024, **464**, 141762.
- 750 12. L. Stasiak-Róžańska, A. Berthold-Pluta, A. S. Pluta, K. Dasiewicz and M. Garbowska,
751 *International Journal of Environmental Research and Public Health*, 2021, **18**, 1108.
- 752 13. K. V. M. Rameez, P. Santhoshkumar, K. S. Yoha and J. A. Moses, *Current Research in*
753 *Nutrition and Food Science Journal*, 2024, **12**, 539–560.
- 754 14. W. K. Ding and N. P. Shah, *Journal of Food Science*, 2009, **74**.
- 755 15. M. Chávarri, I. Marañón, R. Ares, F. C. Ibáñez, F. Marzo and M. Del Carmen Villarán,
756 *International Journal of Food Microbiology*, 2010, **142**, 185–189.
- 757 16. D. Dahiya and P. S. Nigam, *Fermentation*, 2022, **8**, 303.



- 758 17. M. Pateiro, B. Gómez, P. E. S. Munekata, F. J. Barba, P. Putnik, D. B. Kovačević and J. M. Lorenzo, *Molecules*, 2021, **26**, 1547. View Article Online
DOI: 10.1039/D5FB00833F
- 759
- 760 18. E. J. Jeyaraj, Y. Y. Lim and W. S. Choo, *Scientific Reports*, 2022, **12**, 14890
- 761 19. A. Menconi, G. Kallapura, J. D. Latorre, M. J. Morgan, N. R. Pumford, B. M. Hargis and
762 G. Tellez, *Bioscience of Microbiota Food and Health*, 2014, **33**, 25–30.
- 763 20. C. A. Okafor and P. E. Ekwueme, *Asian Food Science Journal*, 2024, **23**, 95–104.
- 764 21. B. Tilahun, A. Tesfaye, D. Muleta, A. Bahiru, Z. Terefework and G. Wessel,
765 *International Journal of Food Science*, 2018, **2018**, 1–7.
- 766 22. G. C. V. Gamage, Y. Y. Lim and W. S. Choo, *Frontiers in Plant Science*, 2021, **12**,
767 792303.
- 768 23. S. Chakraborty, S. Sahoo, A. Bhagat and S. Dixit, *Zenodo (CERN European*
769 *Organization for Nuclear Research)*, 2017, **5**, 197-208
- 770 24. H. Choukaife, A. A. Doolaanea and M. Alfatama, *Pharmaceuticals*, 2020, **13**, 335.
- 771 25. D. Arepally, R. S. Reddy and T. K. Goswami, *Food & Function*, 2020, **11**, 8694–8706.
- 772 26. M. Cassayre, D. T. De Souza, M. Claeys-Bruno, A. Altié, P. Piccerelle and C. Sauzet,
773 *Nanomaterials*, 2025, **15**, 1034.
- 774 27. M. S. Blois, *Nature*, 1958, **181**, 1199–1200.
- 775 28. Md. M. Rahman, Md. B. Islam, M. Biswas and A. H. M. K. Alam, *BMC Research Notes*,
776 2015, **8**, 621
- 777 29. N. Soltani, S. Abbasi, S. Baghaeifar, E. Taheri, M. F. S. Jadid, P. Emami, K. Abolhasani
778 and F. Aslanshirzadeh, *Biotechnology Reports*, 2022, **36**, e00760.
- 779 30. M. A. Ehrmann, P. Kurzak, J. Bauer and R. F. Vogel, *Journal of Applied Microbiology*,
780 2002, **92**, 966–975.
- 781 31. U. Akmal, I. Ghorri, A. M. Elsbali, B. Alharbi, A. Farid, A. S. Alamri, M. Muzammal, S.
782 M. B. Asdaq, M. a. E. Naiel and S. Ghazanfar, *Fermentation*, 2022, **8**, 328.



- 783 32. K. Thinkohkaew, N. Aumphaiphensiri, T. Tangamornsiri, N. Niamsiri, P. Potiyaraj and P. View Article Online
DOI: 10.1039/D5FB00833F
784 Suppavorasatit, *Journal of Agriculture and Food Research*, 2024, **18**, 101405.
- 785 33. Abbas, Z., Hassan, M.A., Huang, W., Yu, H., Xu, M., Chang, X., Fang, X., Liu, L., 2024.
786 Influence of magnesium oxide (MgO) nanoparticles on maize (*Zea mays* L.). *Agronomy*
787 14 (3), 617. <https://doi.org/10.3390/agronomy14030617>.
- 788 34. S. P. Fling and D. S. Gregerson, *Analytical Biochemistry*, 1986, **155**, 83–88.
- 789 35. Y. Liu, M. Grimm, W.-T. Dai, M.-C. Hou, Z.-X. Xiao and Y. Cao, *Acta Pharmacologica*
790 *Sinica*, 2019, **41**, 138–144.
- 791 36. G. Rozos, C. Voidarou, E. Stavropoulou, I. Skoufos, A. Tzora, A. Alexopoulos and E.
792 Bezirtzoglou, *Frontiers in Microbiology*, 2018, **9**, 517.
- 793 37. S. G and S. P. M, *Journal of Advanced Scientific Research*, 2023, **14**, 40–49.
- 794 38. Neda GD, Rabeta MS, Ong MT, *Int Food Res J*, 2013, **20**, 1229–1234.
- 795 39. Deshmukh PR, Joshi A, Vikhar C, Khadabadi SS, Tawar M, *Syst. Rev. Pharm*, 2022, **13**, 685-93.
- 796 40. Y. Pérez-Pacheco, B. Tylkowski and R. García-Valls, *Molecules*, 2025, **30**, 252.
- 797 41. M. Afzaal, F. Saeed, M. Saeed, M. Azam, S. Hussain, A. A. Mohamed, M. S. Alamri and
798 F. M. Anjum, *International Journal of Food Properties*, 2020, **23**, 1899–1912.
- 799 42. Weng, L., Wu, L., Guo, R., Ye, J., Liang, W., Wu, W., Chen, L., & Yang, D., *Journal of*
800 *Nanobiotechnology*, 2022, 20(1). <https://doi.org/10.1186/s12951-022-01563-x>
- 801 43. Barrera-Necha, L. L., Correa-Pacheco, Z. N., Bautista-Baños, S., Hernández-López, M.,
802 Jiménez, J. E. M., & Mejía, A. F. M *Advances in Microbiology*, 2018. 08(04), 286–296.
803 <https://doi.org/10.4236/aim.2018.84019>
- 804 44. M. A. Ahghari, M. R. Ahghari, M. Kamalzare and A. Maleki, *Scientific Reports*, 2022,
805 **12**, 10491.
- 806 45. S. Vijayaram, R. Sinha, C. Faggio, E. Ringø and C.-C. Chou, *AIMS Microbiology*, 2024,
807 **10**, 986–1023.



- 808 46. J. J. Joseph, D. Sangeetha and T. Gomathi, *International Journal of Biological*
809 *Macromolecules*, 2015, **82**, 952–958. View Article Online
DOI: 10.1039/D5FB00833F
- 810 47. S. S. Kumar and S. S. Mohideen, *Scientific Reports*, 2024, **14**, 21182.
- 811 48. M. C. Curk, F. Peledan and J. C. Hubert, *FEMS Microbiology Letters*, 1994, **123**, 241–
812 248.
- 813 49. R. V. Mathai, J. C. Mitra and S. K. Sar, *RASAYAN Journal of Chemistry*, 2021, **14**, 1423–
814 1434.
- 815 50. S. S. Kumar and S. S. Mohideen, *Scientific Reports*, 2024, **14**, 21182.
- 816 51. R. Shanmugam, T. Munusamy, S. Jayakodi, K. A. Al-Ghanim, M. Nicoletti, N.
817 Sachivkina and M. Govindarajan, *Fermentation*, 2023, **9**, 413.
- 818 52. S. K. R. Namasivayam, M. Manohar, J. A. Kumar, K. Samrat, A. Kande, R. S. A.
819 Bharani, C. Jayaprakash and S. Lokesh, *Environmental Research*, 2022, **212**, 113386.
- 820 53. Y. Zhang, Y. Wu, M. Yang, G. Zhang and H. Ju, *Materials*, 2021, **14**, 5538.
- 821 54. P. Hong, S. Li, C. Ou, C. Li, L. Yang and C. Zhang, *Journal of Applied Polymer Science*,
822 2007, **105**, 547–551.
- 823 55. N. Soltani, S. Abbasi, S. Baghaeifar, E. Taheri, M. F. S. Jadid, P. Emami, K. Abolhasani
824 and F. Aslanshirzadeh, *Biotechnology Reports*, 2022, **36**, e00760.
- 825 56. G. I. Edo, A. N. Mafe, Nawar. F. Razooqi, E. C. Umelo, T. S. Gaaz, E. F. Isoje, U. A.
826 Igbuku, P. O. Akpoghelie, R. A. Opiti, A. E. A. Essaghah, D. S. Ahmed, H. Umar and D.
827 U. Ozsahin, *Designed Monomers & Polymers*, 2024, **28**, 1–34.
- 828 57. N. Sulistiani, I. Novarina, N. Inawati, A. Dinoto, H. Julistiono, R. Handayani and S.
829 Saputra, *IOP Conference Series Earth and Environmental Science*, 2020, **572**, 012026.
- 830 58. A. Varela-Pérez, O. O. Romero-Chapol, A. G. Castillo-Olmos, H. S. García, M. L.
831 Suárez-Quiroz, J. Singh, C. Y. Figueroa-Hernández, R. Viveros-Contreras and C. Cano-
832 Sarmiento, *Foods*, 2022, **11**, 740.



- 833 59. J. Arratia-Quijada, K. Nuño, V. Ruíz-Santoyo and B. A. Andrade-Espinoza, *Journal of*
834 *Functional Foods*, 2024, **116**, 106192. View Article Online
DOI: 10.1039/D5FB00833F
- 835 60. A. A. Argyri, G. Zoumpopoulou, K.-A. G. Karatzas, E. Tsakalidou, G.-J. E. Nychas, E. Z.
836 Panagou and C. C. Tassou, *Food Microbiology*, 2012, **33**, 282–291.
- 837 61. S. S. Kumar and S. S. Mohideen, *Scientific Reports*, 2024, **14**, 21182.
- 838 62. S. Nigam, D. V. Ram and A. a. M. Kumar, *International Journal of Pharmaceutical*
839 *Sciences Review and Research*, 2022, 154–160.
- 840 63. M. A. O. Torio, M. Adachi, R. N. Garcia, K. Prak, N. Maruyama, S. Utsumi and E. M.
841 Tecson-Mendoza, *Food Research International*, 2011, **44**, 2984–2990.
- 842 64. Ma. C. Gamis, L. Y. Uy, A. Laurena, W. Hurtada and M. A. Torio, *Applied Sciences*,
843 2020, **10**, 8787.
- 844 65. I. M. Fareez, S. M. Lim, R. K. Mishra and K. Ramasamy, *International Journal of*
845 *Biological Macromolecules*, 2014, **72**, 1419–1428.
- 846 66. M. Hidalgo, M. J. Oruna-Concha, S. Kolida, G. E. Walton, S. Kallithraka, J. P. E.
847 Spencer, G. R. Gibson and S. De Pascual-Teresa, *Journal of Agricultural and Food*
848 *Chemistry*, 2012, **60**, 3882–3890.



Figures

View Article Online
DOI: 10.1039/D5FB00833F

Fig. 1 *C. ternatea* extract coated chitosan- *L. acidophilus* Nano-encapsule
(CT-CS-LA-NC)

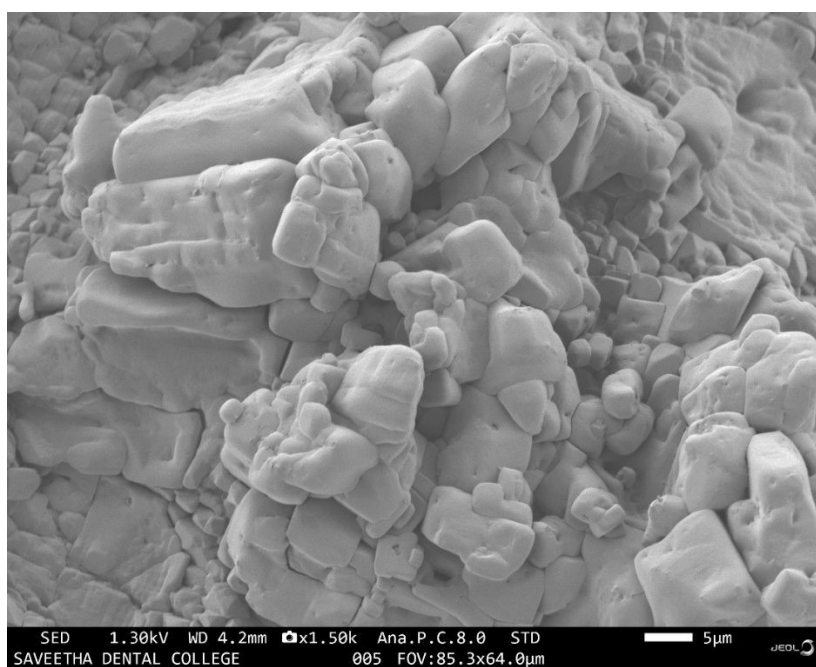


Fig. 2 SEM Micrograph of CT-CS-LA-NC

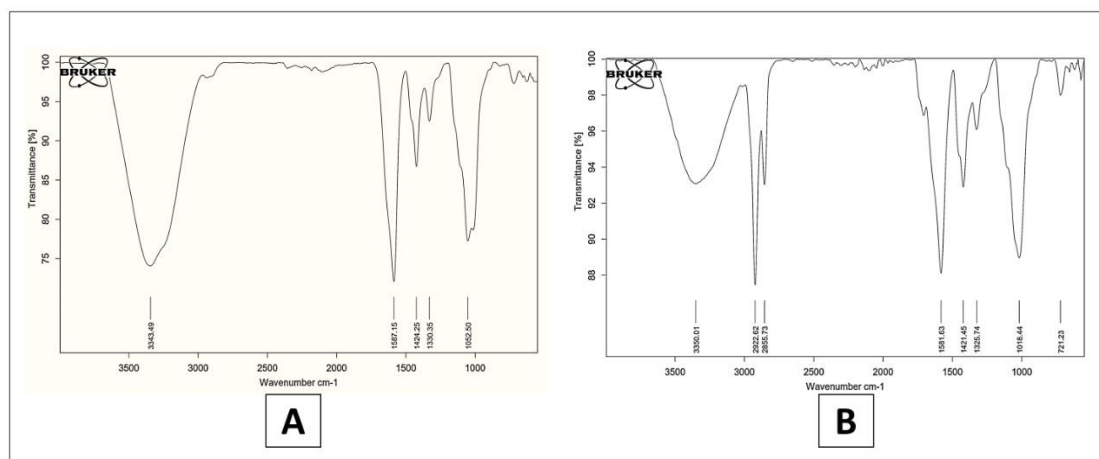


Fig. 3 FTIR Spectrum of FTIR Spectrum of (A) CS-NC (B) CT-CS-LA-NC

View Article Online

DOI: 10.1039/D5FB00833F

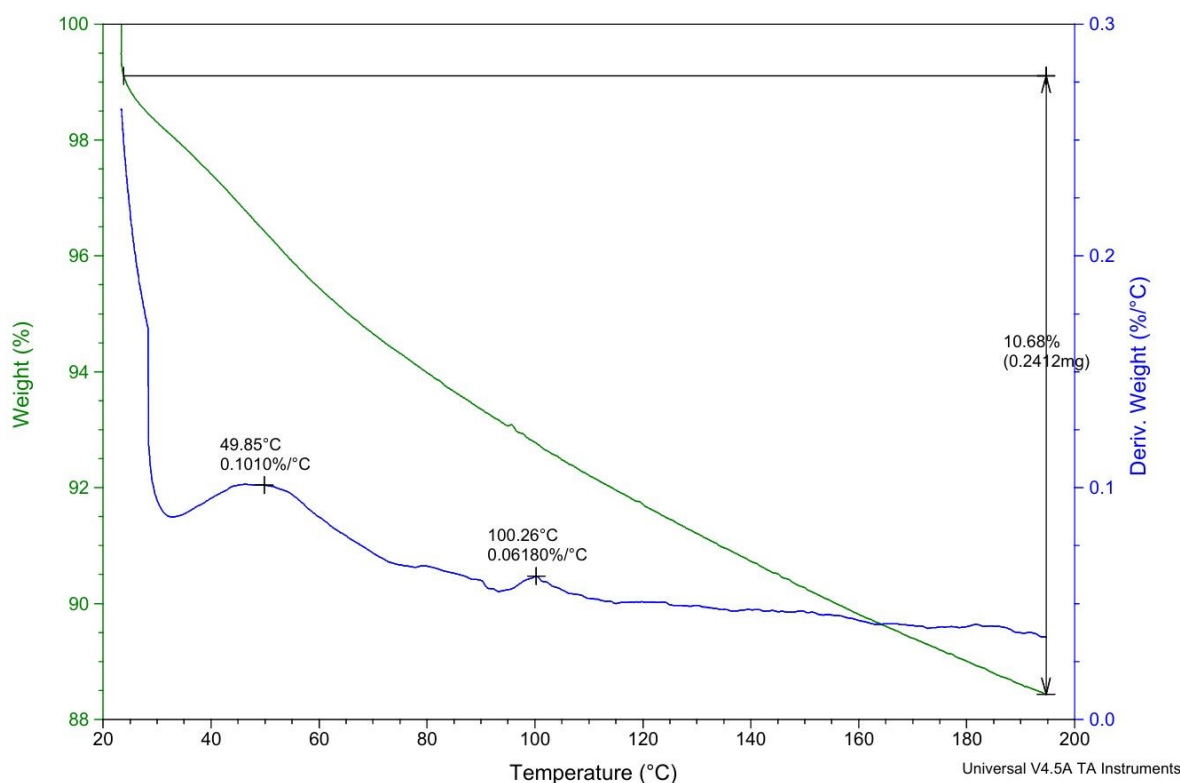


Fig. 4 TGA Analysis of CT-CS-LA-NC

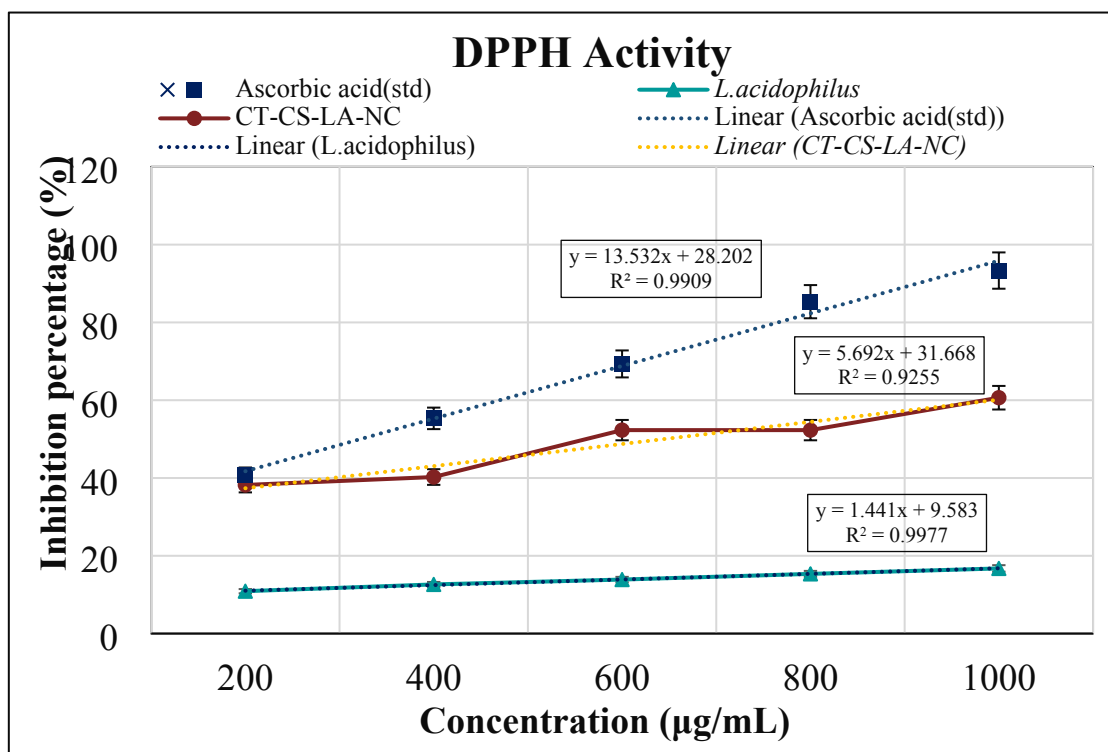


Fig. 5 DPPH assay of CT-CS-LA-NC

(Values are presented as the mean \pm standard error of the mean (n = 3). Significance at < 0.05)



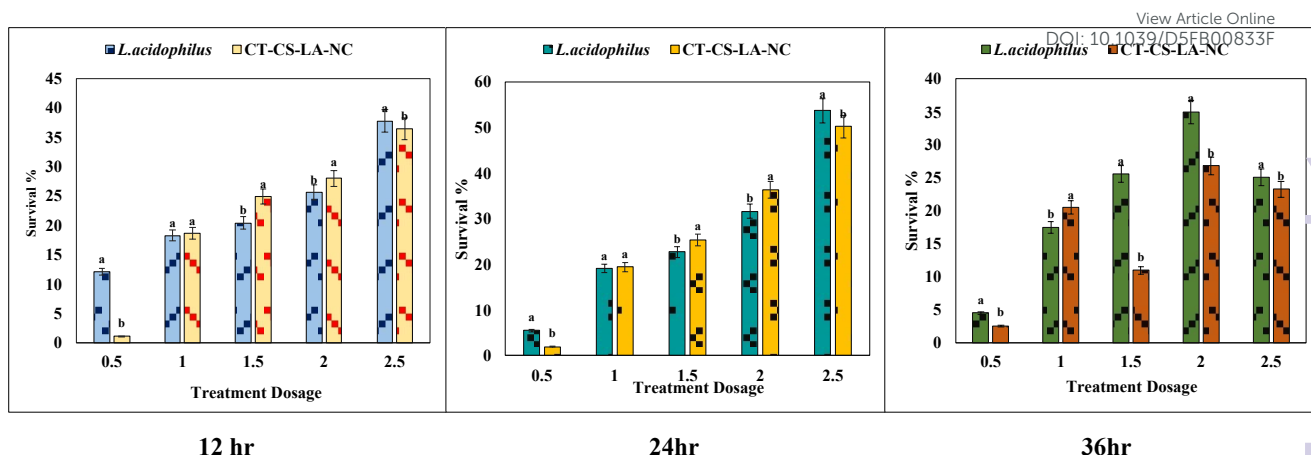


Fig. 6 Viability of free *L. acidophilus* & CT-CS-LA-NC at pH 2.5 at different time intervals (12, 24, and 36 hr). The X-axis represents the treatment dosage added to 100 ml of MRS broth. For *L. acidophilus*, dosages are 0.5 - 2.5 ml. For CT-CS-LA-NC, dosages are 0.5-2.5 g.

(Values are presented as the mean \pm standard error of the mean (n = 3). Different letters denote statistical significance ($P < 0.05$) according to Duncan's multiple range test, which was performed following a significant one-way ANOVA)

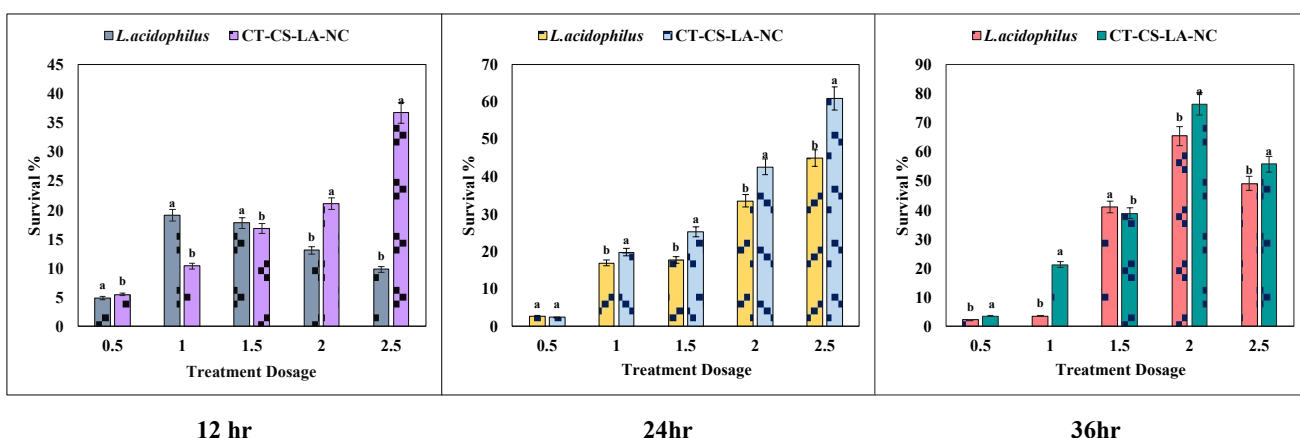


Fig. 7 Viability of free *L. acidophilus* & CT-CS-LA-NC at pH 3.5 at different time intervals (12, 24, and 36 hr). The X-axis represents the treatment dosage added to 100



ml of MRS broth. For *L. acidophilus*, dosages are 0.5 - 2.5 ml. For CT-CS-LA-NC, dosages are 0.5-2.5 g.

View Article Online
DOI: 10.1039/D5FB00833F

(Values are presented as the mean \pm standard error of the mean (n = 3). Different letters denote statistical significance (P < 0.05) according to Duncan's multiple range test, which was performed following a significant one-way ANOVA)

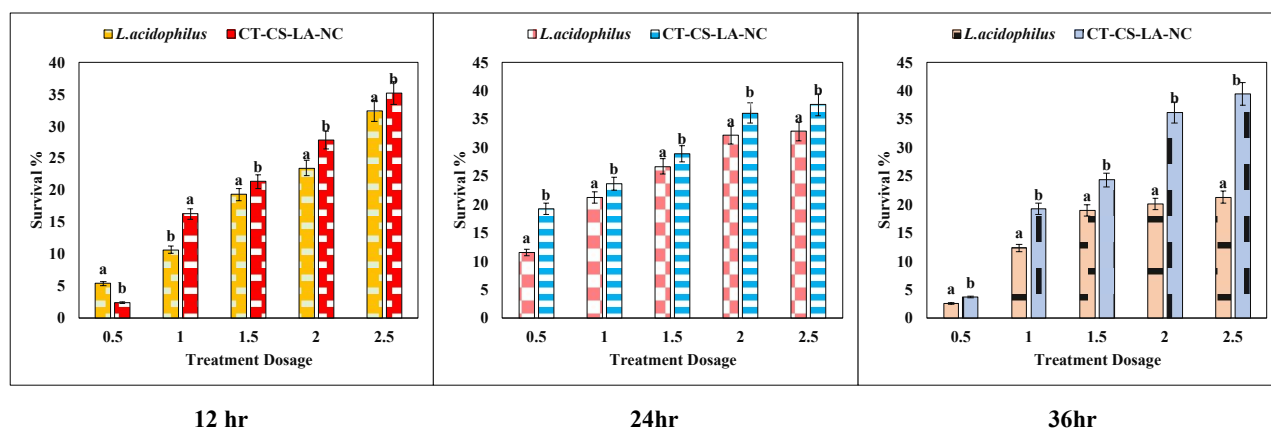
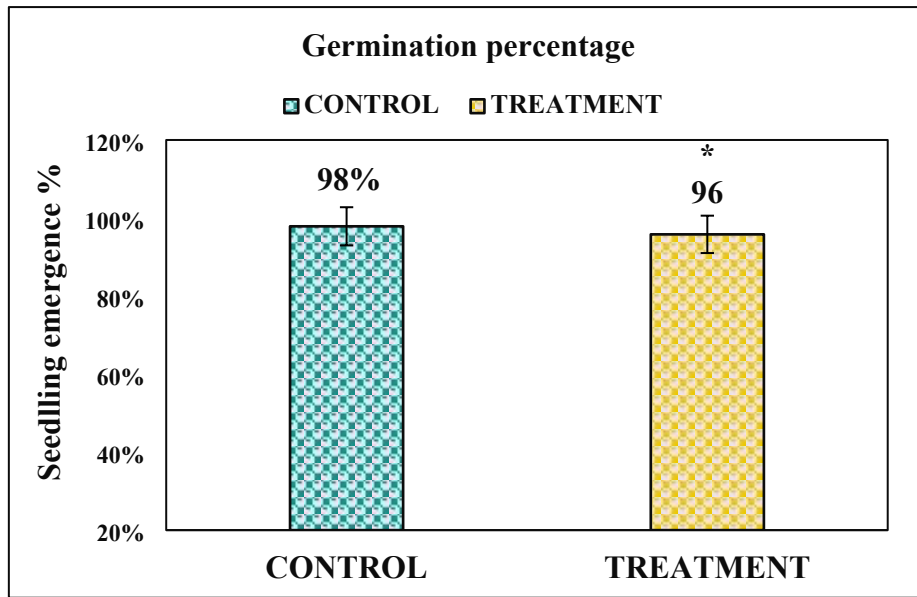


Fig. 8 Viability of free *L. acidophilus* & CT-CS-LA-NC at pH 7.5 at different time intervals (12, 24, and 36 hr). The X-axis represents the treatment dosage added to 100 ml of MRS broth. For *L. acidophilus*, dosages are 0.5 - 2.5 ml. For CT-CS-LA-NC, dosages are 0.5-2.5 g.

(Values are presented as the mean \pm standard error of the mean (n = 3). Different letters denote statistical significance (P < 0.05) according to Duncan's multiple range test, which was performed following a significant one-way ANOVA)





View Article Online
DOI: 10.1039/D5FB00833F

Fig. 9 Seedling Germination of *Vigna mungo*. Significance at (*P < 0.05)

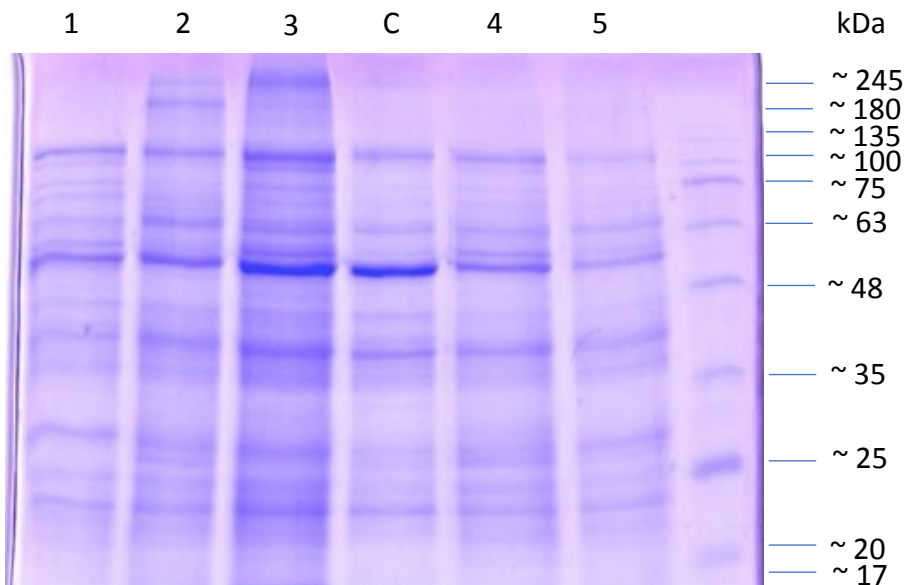


Fig. 10 SDS-PAGE analysis of protein extracted from *Vigna mungo*



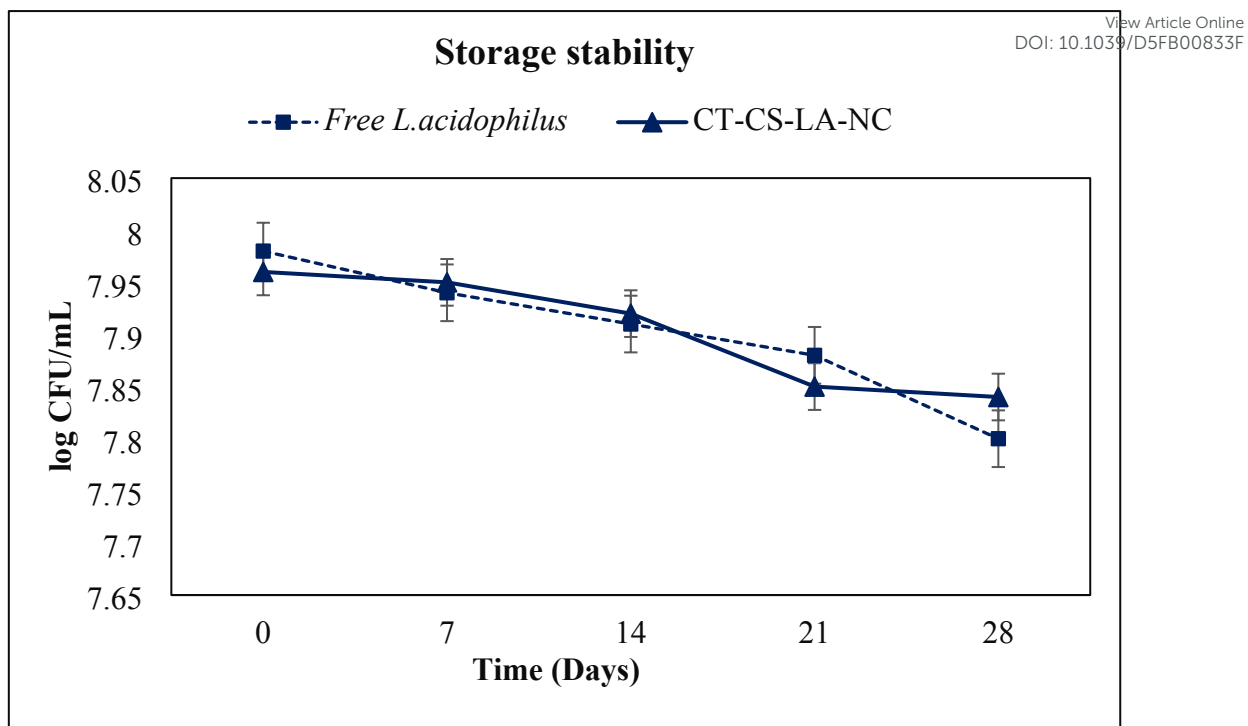
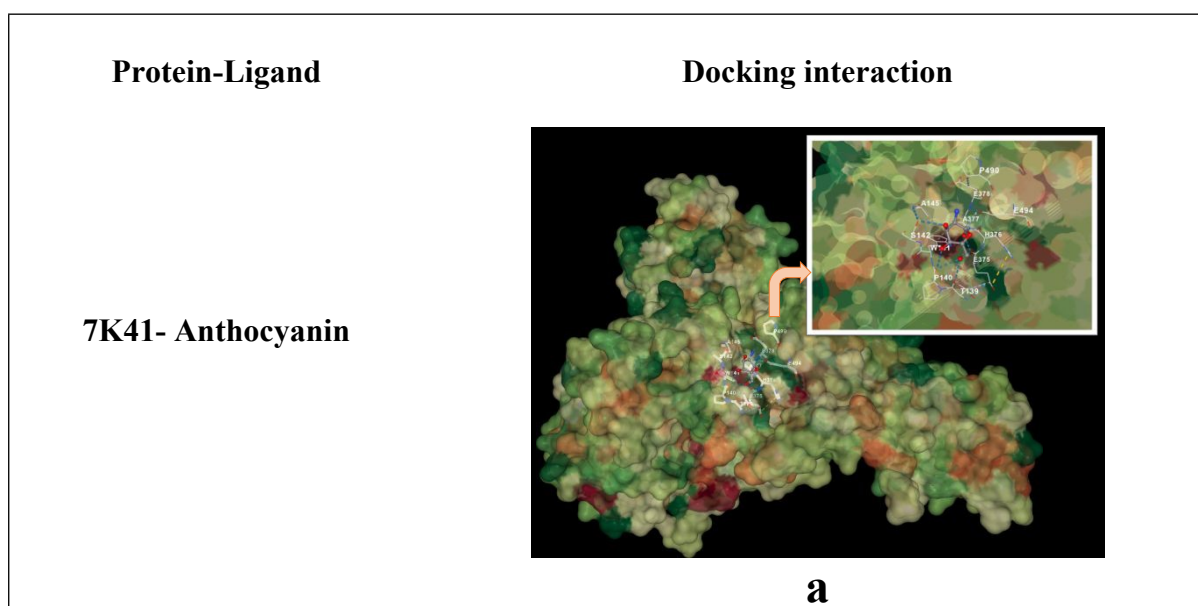
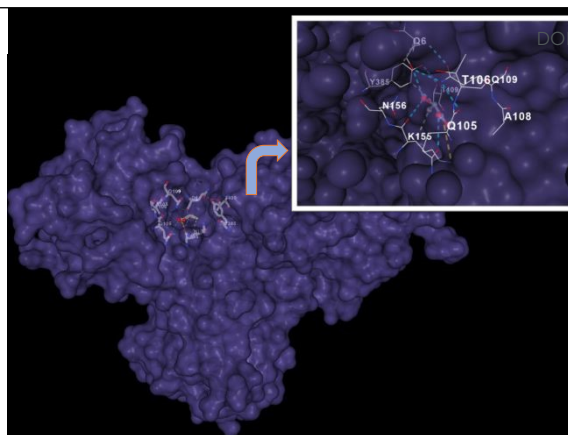
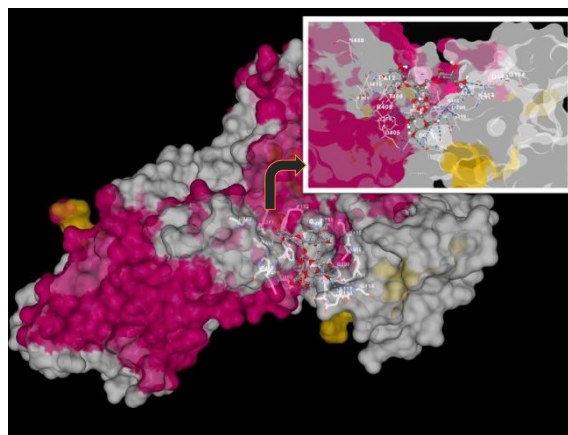
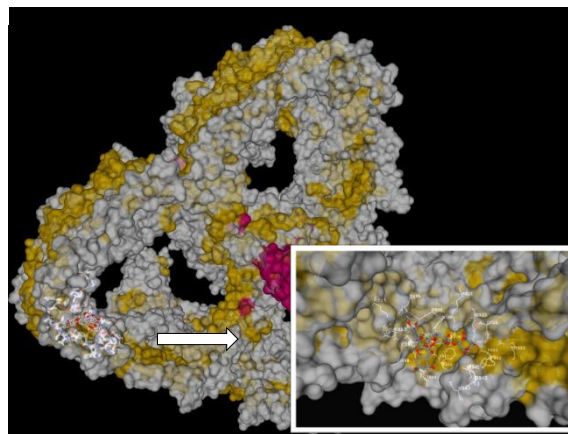


Fig. 11 Storage stability of free *L. acidophilus* and CT-CS-LA-NC at 4°C for 28 days. The presented values are expressed as means \pm SD (n = 3).



7K41- Lactic acid**b****7K41- Chitosan****c****8AE1- Anthocyanin****d**

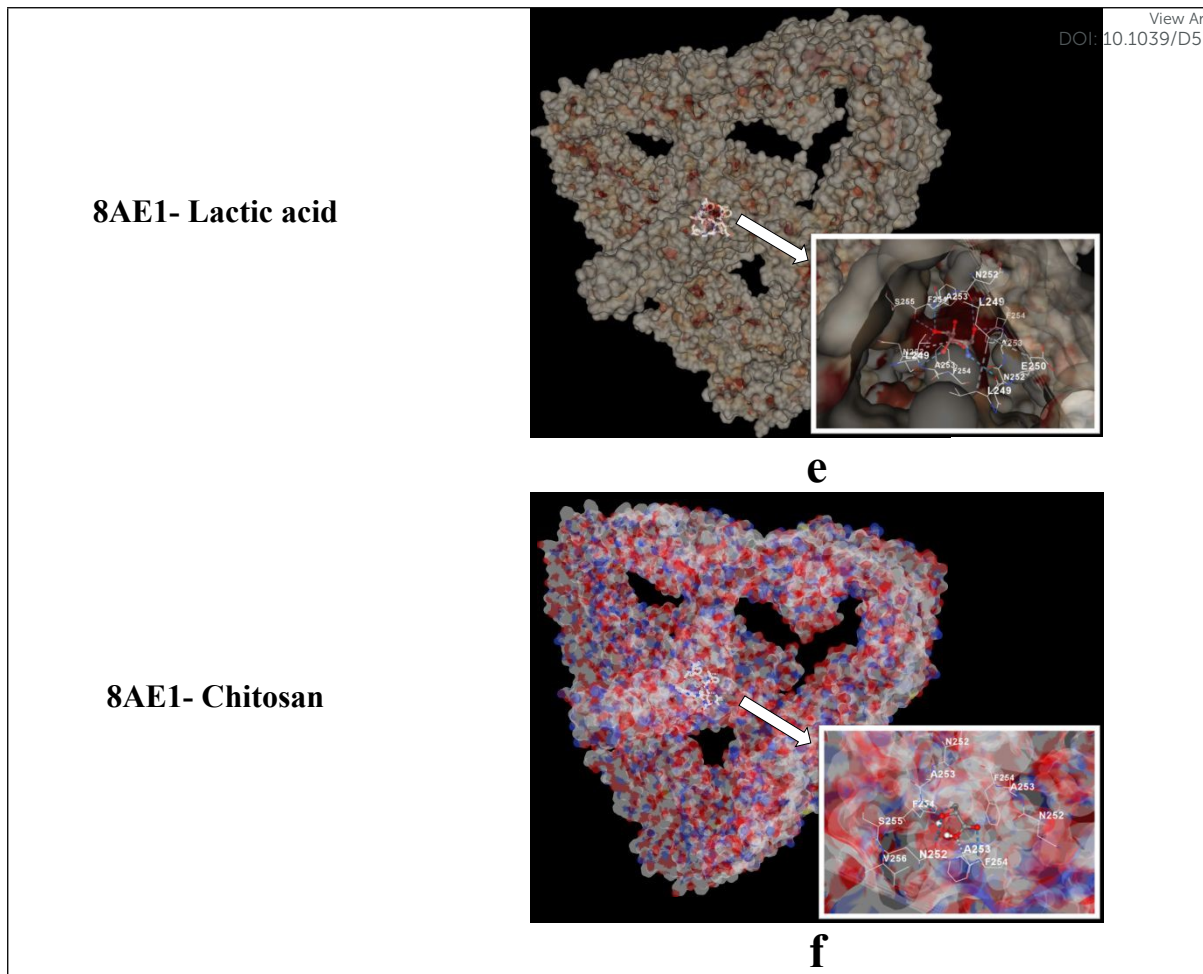


Fig. 12 *In-silico* docking interaction of proteins (7K41, 8AE1) with ligands (Anthocyanin, Lactic acid, and Chitosan)



Tables

View Article Online
DOI: 10.1039/D5FB00833F**Table. 1 Morphological and biochemical characteristics of *L.acidophilus***

Characterization	Result
Gram staining	Gram Positive
Spore Test	Non- spore forming rods
Motility test	Non motile
Indole production test	Negative
Catalase test	Negative

Table. 2 Qualitative analysis of the plant extracts of *Clitoria ternatea* to screen for the presence of phytochemicals.

S. No	Phytochemicals analysis	Presence/Absence
1.	Alkaloids	+
2.	Flavonoids	+
3.	Steroids	-
4.	Phenol	+
5.	Tannin	+
6.	Saponin	-



Table.3 Antibacterial activity of Free *L. acidophilus* and Nano-encapsulated *L. acidophilus* against *Escherichia coli* and *Bacillus subtilis*

View Article Online

DOI: 10.1039/D5FB00833F

S.NO	Treatment	Zone of inhibition (mm)	
		<i>Escherichia coli</i> (ATCC 25922)	<i>Bacillus subtilis</i> (ATCC 6051)
1.	Free <i>L. acidophilus</i>	12 ± 0.19 ^c	13 ± 0.19 ^c
2.	Nano-encapsulated <i>L. acidophilus</i>	14.2 ± 0.26 ^a	15.1 ± 0.24 ^a
3.	Secretory product of free <i>L. acidophilus</i>	13.1 ± 0.17 ^b	13.4 ± 0.21 ^c
4.	Secretory product of Nanoencapsulated <i>L. acidophilus</i>	14.3 ± 0.27 ^a	14.4 ± 0.32 ^b

(Values are presented as the mean ± standard error of the mean (n = 3). Different letters in the same columns denote statistical significance (P < 0.05) according to Duncan's multiple range test, which was performed following a significant one-way ANOVA)

Table. 4 *In-silico* Docking analysis of proteins and ligands using CB-Dock

Protein	Ligand	Interaction score (kcal/mol)	Cavity volume
7K41	Anthocyanin	-9.4	2633
7K41	Lactic acid	-4.1	2633
7K41	Chitosan	-5.2	534
8AE1	Anthocyanin	-9.6	893
8AE1	Lactic acid	-3.8	2141
8AE1	Chitosan	-5.4	2163



Availability of data and materials

The data will be made available on request from the authors

